Ultrasonic Data Testing of Time-Lapse Tomography

D.D. Šijačić, J. Spetzler and K.H.A.A. Wolf, Delft University of Technology, The Netherlands*

SUMMARY

This paper is a validation study of a time-lapse tomographic method using ultrasonic broadband waveform data recorded in a crosswell tomographic laboratory experiment. Two data sets have been obtained from two almost identical physical models simulating pre-flood and post-flood stages during an enhanced oil recovery. We have applied a time-lapse method based on ray theory and wave scattering theory to estimate velocity differences thereby induced. Our objective is to develop a 4D crosswell tomography and to validate it with ultrasonic data. The variations of the time-lapse tomographic method, i.e., how the observed traveltimes shifts are estimated and which type of inversion (ray of wave theory based) is used, produce four different time-lapse velocity tomograms. Lastly, applications of our 4D method on real field data sets, and on a new ultrasonic experiment simulating CO_2 injection in the subsurface, are discussed.

INTRODUCTION

We investigate time-lapse (also known as 4D) tomography - a seismic monitoring technique. The word *tomography* is composed of the Greek words *tomos* meaning *a slice* and *graphi* that is translated to *write on*. Accordingly, acoustic monitoring by seismic tomography refers to the method in the academic field of seismology and the industrial area of exploration seismology where primarily compressional waves (i.e., sound waves) are used to compile images of the geology. In contrast to log data, seismic tomography provides information about the subsurface away from the wells.

Seismic data recorded in seismic experiments contain mostly low-frequency components because the Earth acts as a low-pass filter. High-resolution velocity models estimated in inversions based on ray theory may be considerably biased because ray theory is a high-frequency approximation of the wave theory. To obtain correct high-resolution images, it is instead better to apply tomographic inversion methods based on wave theory, because the finite-frequency effect of waves is taken into account.

First, we present a linear wave theory that we use in a time-lapse tomographic wavefield inversion. Thereafter, an ultrasonic experiment from the University of Durham is described. The ultrasonic waveform data from the Durham experiment is used to validate our 4D tomographic method. Images with the estimated time-lapse velocity, compiled with difference variations of our 4D monitoring approach, are shown. Finally, we draw conclusions and discuss possible seismic applications of this method.

LINEAR FINITE-FREQUENCY WAVEFIELD THEORY

In this section, we present a linear finite-frequency wave theory (also called scattering theory) for the traveltime variation of propagating wavefields in complex media wherein single scattering of waves is included. Complex heterogeneous media may have anomalies smaller in size than the Fresnel zone. We use the first-order Rytov approximation to model wavefields, wherein only differences in P-wave velocities are taken into account (shear waves are neglected as well as variations in densities). The Rytov wavefield $P_R(\mathbf{r}_r,\mathbf{r}_s,\omega)$ at the angular frequency $\omega = 2\pi\nu$ emitted from the source position $\mathbf{r}_s$ and recorded at the receiver position $\mathbf{r}_r$ is given by

$$P_R(\mathbf{r}_r,\mathbf{r}_s,\omega) = P_0(\mathbf{r}_r,\mathbf{r}_s,\omega)\exp\left(\frac{P_B}{P_0}(\mathbf{r}_r,\mathbf{r}_s,\omega)\right), \tag{1}$$

where $P_0(\mathbf{r}_r,\mathbf{r}_s,\omega)$ is the reference wavefield inherent to the reference velocity model $v_0(\mathbf{r})$. $P_B(\mathbf{r}_r,\mathbf{r}_s,\omega)$ is the first order Born wavefield given by

$$P_B(\mathbf{r}_r,\mathbf{r}_s,\omega) = \int_V \frac{2\Delta v(\mathbf{r})\omega^2}{v_0^3(\mathbf{r})} P_0(\mathbf{r}_r,\mathbf{r}_s,\omega)G(\mathbf{r}_r,\mathbf{r}_s,\omega)dV, \tag{2}$$

where $G(\mathbf{r}_r,\mathbf{r}_s,\omega)$ is far-field Green's function in an arbitrary reference medium [Snieder and Lomax (1996)] and $\Delta v(\mathbf{r})$ denotes the velocity perturbation field. The Rytov wavefield accounts for the single-scattering process of a propagating wavefield in heterogeneous media, for more details in derivation, see Aki and Richards (1980); Woodward (1992); Snieder and Lomax (1996); Spetzler and Snieder (2001).

The traveltime shift $\Delta t(\mathbf{r}_r,\mathbf{r}_s)$ and amplitude variation $\Delta A/A_0(\mathbf{r}_r,\mathbf{r}_s)$ of the scattered field with respect to the reference field are derived from the real and imaginary part, respectively, of the exponential function in Eq. (1). To the first order of the approximation (i.e., a single-scattering approach), the traveltime delay is given by

$$\Delta t(\mathbf{r}_r,\mathbf{r}_s) = \int_V \Delta v(\mathbf{r})K_{\Delta t}(\mathbf{r})dV, \tag{3}$$

while the relative amplitude variation is

$$\frac{\Delta A}{A_0}(\mathbf{r}_r,\mathbf{r}_s) = \int_V \Delta v(\mathbf{r})K_{\Delta A}(\mathbf{r})dV. \tag{4}$$

The sensitivity functions $K_{\Delta t}(\mathbf{r})$ and $K_{\Delta A}(\mathbf{r})$ are known as Fréchet kernels for the traveltime shift and amplitude variation. The Fréchet kernel depends on the source-receiver geometry, and the reference model, and includes the broadband frequency characteristics of the recorded wavefield. The integration is carried out over the volume V between the source and receiver. A detailed derivation of Eq. (3) and (4) is given by Aki and Richards (1980), Snieder and Lomax (1996) and Spetzler and Snieder (2001).

For wave propagation in 2D, the Fréchet kernel for traveltime shift is described by

$$\begin{aligned} K_{\Delta t}^{2D}(x,z) \quad = \quad & -\sqrt{\frac{L}{v_0^5 x(L-x)}}\int_{\nu_0-\Delta\nu}^{\nu_0+\Delta\nu} A(\nu) \\ & \times\sqrt{\nu}\sin\left(\frac{\nu\pi L z^2}{v_0 x(L-x)}+\frac{\pi}{4}\right)d\nu, \end{aligned} \tag{5}$$

in a homogeneous reference medium of the constant velocity v_0 and with the 2D coordinate $\mathbf{r} = (x,y)$. The source-receiver distance $L = |\mathbf{r}_r - \mathbf{r}_s|$, and the frequency is denoted by ν. The sensitivity kernel is integrated over the frequency band $[\nu_0-\Delta\nu;\nu_0+\Delta\nu]$ and the normalised amplitude spectrum $A(\nu)$ satisfies $\int_{\nu_0-\Delta\nu}^{\nu_0+\Delta\nu} A(\nu)\,d\nu = 1$. Further on in this paper, we discuss only traveltime components, though in a similar way, amplitude components can be easily derived too (plots of sensitivity kernels for amplitude perturbations can be found in Aki and Richards (1980); Snieder and Lomax (1996)). Here, we constrain our validation study only to traveltime tomography because the travel time attribute is more reliable than the amplitude attribute (i.e., possible unknown parameters are the source-receiver coupling, attenuation and the geometrical spreading factor).

For 3D wave propagation in a homogeneous reference model, the Fréchet kernel for traveltime residuals is equal to

$$\begin{aligned} K_{\Delta t}^{3D}(x,y,z) \quad = \quad & -\frac{L}{v_0^3 x(L-x)}\int_{\nu_0-\Delta\nu}^{\nu_0+\Delta\nu} A(\nu) \\ & \times\nu\sin\left(\nu\pi L\frac{(y^2+z^2)}{v_0 x(L-x)}\right)d\nu, \end{aligned} \tag{6}$$

where the 3D coordinate $\mathbf{r} = (x, y, z)$. This equation can also be found in Hung *et al*. (2001) and Spetzler *et al*. (2002).

In a similar vein to Eq. (3), the traveltime shift derived from ray theory is a line integration of the slowness perturbation field along the ray path jointing the source and receiver point. One can derive the ray theoretical result for traveltime shifts from Eq. (3) because the Fréchet kernel $K(\mathbf{r})$ converges to a delta function in the high-frequency limit. Thereby, the volume integration is reduced to a line integration. As can be seen, for the construction of the finite-frequency Fréchet kernel, a given reference velocity model, the source-receiver geometry and the power-spectrum of the recorded wavefield must be known. An example of sensitivity kernels for transmitted waves in a crosswell configuration is illustrated in Fig. 1. The sensitivity kernels (shades of blue, white and red) are smooth functions since the finite-frequency effect of waves is taken into account. The Fresnel zones (edge of the white and blue colour) for the finite-frequency waves and the ray paths (solid yellow line) are also visible in the figure. The Fresnel zones correspond well to the central width of the sensitivity kernels. Because of the high-frequency approximation applied in ray theory, the sensitivity to slowness perturbations vanishes at positions off the ray path.

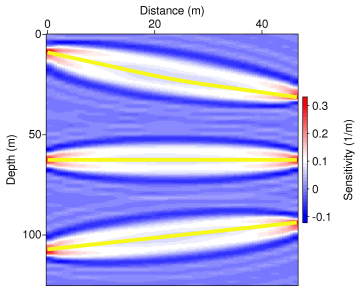

Figure 1: An example of Fréchet kernels calculated within finite-frequency wave theory and of ray paths in a crosswell setting for the case of the Durham ultrasonic experiment.

Scattering theory for traveltimes of waves is important in media where the Fresnel zone $L_F = \sqrt{\lambda L}$ is larger than the length-scale a of heterogeneities. (λ is the dominant wavelength and L denotes the length of the ray path.) Hence,

$$\frac{L_F}{a} > 1. \qquad (7)$$

An illustration of the validity of expression (7) can be found in Fig. 4 and 5 of Spetzler and Snieder (2001).

There is a clear distinction between scattering theory for the traveltime of waves propagating in 2D and 3D media. For wave propagation in 3D, it turns out that the sensitivity to slowness perturbations on the ray path vanishes. This is a counter-intuitive result compared to ray theory that predicts non-zero sensitivity to the slowness perturbation field on the ray only. In addition, finite-frequency theory for the traveltime of waves has the maximum sensitivity to slowness perturbations away from the ray path both for wave propagation in 2D and 3D. In Fig. 1 of Spetzler et al. (2002), cross sections of 2D and 3D Fréchet kernel for transmitted waves are illustrated. For 3D wave propagation in 2.5 dimensional velocity media, it is sufficient to apply finite-frequency wave theory for 2D wave propagation. Physically speaking, the scattering process in the direction of constant velocity ensures that the 3D finite-frequency wave theory converges to a 2D scattering formulation which mathematically can be proved with the stationary phase theory.

ULTRASONIC TIME-LAPSE EXPERIMENT

The main objective of this paper is validation of a time-lapse crosswell monitoring method by using ultrasonic data. Ultrasonic broadband waveform data are recorded in the ultrasonic seismic laboratory at the University of Durham where crosswell seismic survey was simulated [Legget et al. (1993); Pratt (1999)]. The physical model (two of them) in Durham experiment consists of seven layers with different epoxy resin mixtures representing plane-layered sedimentary sequence containing a reservoir layer and simple geological structure. The models differed only in the reservoir layer, which was in one case uniform (representing pre-flood stage) and in another it contained post-flood zone (simulating progress of fluids injected in reservoir rocks during enhanced oil recovery process). A cross section of the model(s) is illustrated in Fig. 2 where flood zone in the reservoir layer is indicated by cross-hatched region. Furthermore, Fig. 2 also shows nominal velocities, which are only an indication for the true velocity model since characteristics of epoxy resin are only weak under control. Time-lapse traveltime tomographic imaging technique aims to locate the extent of the flood zone and to accurately detects the velocity change.

Low-frequency transmitted waves were acquired from each model (in a form of two data sets) in a crosswell configuration with two vertical wells. In between the two wells, the velocity model consists of large and small scale structures. For the small-scale velocity structure (thin layer with one channel feature), the theoretical requirements for the application of ray theory are not satisfied. On the contrary, the conditions for the application of finite-frequency wave theory are valid for the whole velocity model in the Durham laboratory experiment. However, the difference between two models - the flood zone can be considered as a large scale structure and therefore, it is expected to be imaged well enough both with ray and wave theory based inversion. The ultrasonic surveys also include realistic noise contributions due to uncertainties in source-receiver positions, in the traveltime estimation and in the estimation of the reference velocity, see Legget et al. (1993). Additionally, two models are used to simulate one configuration in two stages which also impose some errors. The models were intensionally made to be identical, apart from the flood zone, but that can never be completely achieved.

In the ultrasonic experiment, 500 kHz piezoelectric transducers are used as sources and receivers. There are 51 source and receiver positions which results in 2601 recorded traces. The target zone of velocity between the two wells measures 46.5 mm in the offset direction and 125 mm in the depth direction. To simulate a realistic crosswell experiment, all distances, times and frequencies are scaled by a factor 1000. Hence, the lateral length and depth of the target zone has the dimensions 46.5 m$\times$125 m, whereas the frequency of the recorded wavefield is between 200 Hz and 500 Hz.

The Durham laboratory experiment makes use of transmitted waves that propagate in 3D. However, the epoxy model represent a 2.5D velocity medium, since the velocity is constant in the lateral direction perpendicular to the source-receiver plane. In turn, the finite-frequency Fréchet kernels for the transmitted waves are derived from the 2D wave equation.

To locate the flood zone by 4D tomography, there are two equivalent approaches to be applied. One is to perform separate traveltime inversion of data from the baseline survey and data from the monitoring survey, obtain velocity tomograms and then find the difference by subtracting the estimated baseline model from the inverted monitor model. Another, more direct approach is to find the traveltime delays between the first arrivals in the pre-flood model and first arrivals in the post-flood model, invert that and get the image of the time-lapse velocity structure.

To invert one data set, the following steps are carried out: 1) Define a relevant reference model and calculate Fréchet kernels compiled with either finite-frequency wave theory or ray theory, 2) calculate the refer-

ence traveltimes, 3) estimate the traveltime delay between the observed and reference traveltimes, and finally 4) invert the observed traveltime shifts in order to estimate a velocity model between the two wells.

For the time-lapse monitoring, the more direct approach for the inversion consist of one step less. Namely, instead of steps 2) and 3) there is only one: the estimation of the traveltime shift between the baseline and monitor traveltimes. That has been obtained automatically by the crosscorrelation of the recorded waveforms (previously muted and filtered) from the baseline and monitoring survey.

The reference velocity model is obtained assuming that calibrated sonic logs were run in both wells to give an initial estimate of the velocity field between the two wells in a baseline survey (i.e., by the linear interpolation). Therefore, we have used the velocity structure in Fig. 2 only without the thin layer with the channel structure. The parameterisation of the velocity model is a grid by 64 $\times$24 cells of the constant velocity. The Fréchet kernels with respect to the reference model are computed either with scattering theory or ray theory. For the inversion of only one data set, the traveltime delay is estimated as the difference between the observed traveltimes and the reference traveltimes. The reference traveltimes are always calculated for the reference model with ray theory. To compute the observed traveltime delay, observed and reference traveltimes are subtracted from each others. The observed traveltimes are estimated in a correlation analysis of the observed waveforms and the source wavelet where the latter is known from an independent measurement in water. Finally, a common least-squares inversion method is applied in the finite-frequency wave and ray theoretical inversion. It is fair to compare the estimated velocity models compiled with scattering theory and ray theory when the resolution matrices in the two inversion approaches are identical. As has been previously shown by Spetzler (2003a,b), the velocity tomogram compiled by wave theory is with higher resolution compared to the one obtained with ray theory. In addition, because of the limitations of the high-frequency approximation applied in ray theory, the strength of small-scale velocity is underestimated. The breakdown of ray theory is as well clearly demonstrated in Fig. 4 and 5 of Spetzler and Snieder (2001).

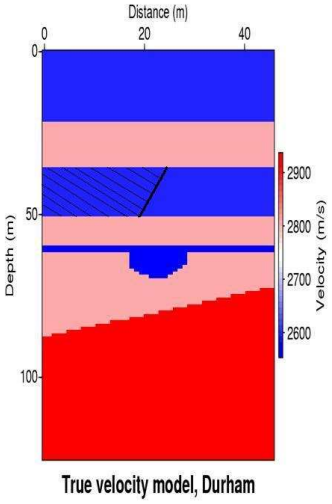

Figure 2: Cross section of the epoxy resin scale model with the indication of the nominal velocities. Additionally, the location of the flood zone is presented by the cross-hatched region.

We show the time-lapse velocity tomograms compiled with the finite-frequency wave theory and the standard ray theory in Fig. 3A and 3B, respectively. We observe only a small difference between these two images. This is expected since the conditions for ray theory are not violated. Still, the time-lapse velocity tomogram obtained by the finite-frequency wave theory seems to be overall less noisy. Practically, the time-lapse physical model in the Durham experiment was obtained by replacing a part of the reservoir layer with a epoxy mixture of lower velocity and greater absorption to simulate a flood zone. The initial reservoir layer (of the epoxy raisin) had the nominal velocity of 2573 m/s while the replaced material had the velocity of 2147 m/s in the post-flooded model. We estimate that the time-lapse velocity change in the reservoir layer is on the order of -400 m/s. Thus, our developed monitoring method gives an accurate estimation of the induced velocity difference. Also, the front of the flooding zone is accurately located.

Fig. 4A shows a difference velocity tomogram obtained simply by subtracting the pre-flood image from the post-flood image (not shown here). Those images were estimated separately by tomographic inversion. The finite-frequency wave theory was used in the inversion step. The traveltime delays are found following the first three steps previously described. The time-lapse tomographic velocity field is consistent with the ones in Fig. 3, but shows much more noise and some additional differences. That is a consequence of two separate and independent inversions where not all parameters and characteristics of the inversions are necessarily the same. The damping parameter is different in order to get similar velocities and consequently, it is difficult to obtain identical chi squared values (the chi squared value is a combination of the data misfit and the model resolution). The 4D result is affected by the velocity differences in the other parts of the model since finite-frequency inversion is more sensitive than the ray theory to preprocessing errors in the observed data. Also, the velocity difference in the flood zone is slightly underestimated. In order to avoid those problems, yet another way of processing has been tested so that 4D image is directly estimated from the inversion of only one data file. Therefore, the third and the final approach we have investigated follows the four steps previously described in the inversion of one data set, with the difference that the reference model is the actual baseline velocity structure (i.e., estimated by inversion). Furthermore, in the last step of the inversion, this baseline velocity structure is subtracted from the estimated perturbation velocity model. The resulting 4D image is presented in Fig. 4B.

The time-lapse tomographic velocity models compiled with the finite-frequency wave theory presented in Fig. 4B can be compared to the result of Legget et al. (1993) presented in Fig. 7C which shows a difference velocity tomogram obtained by ray theory. Again, as expected both results are very similar (only that Fig. 7C is the mirrored image since the true velocity model has mirrored geometry and the source-receiver positions are flip-flopped).

CONCLUSIONS

Using ultrasonic data, we show that traveltime time-lapse tomography is a powerful method for monitoring and has a number of applications.

We proposed to apply a finite-frequency wave theory in time-lapse tomographyc inversion scheme, since it is not affected by the limitations of ray theory. In the contrast to wave theory, ray theory is not valid for the media where the size of the velocity anomalies is smaller than the Fresnel zone.

In the Durham time-lapse ultrasonic experiment, both ray and wave theory give satisfactory estimations of the flood zone in the reservoir (since its size is larger than the Fresnel zone). The process of the traveltimes shift estimation plays an important role and, we conclude that the most correct way to estimate traveltimes shifts is by crosscorrelation of muted data from the baseline and monitoring survey, followed by the application of moving average filter on the estimated time shifts. Inverting the new data file provieds an image free of noise in wich the accurately located flood zone has relatively sharp edges.

Time-lapse tomography combined with the finite-frequency wave the-

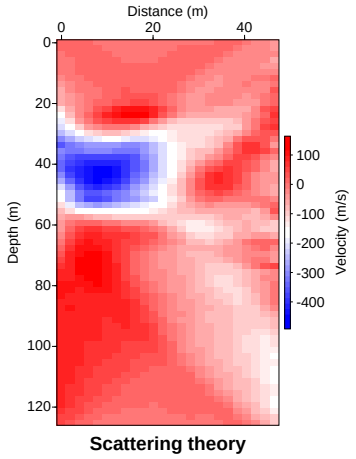

A)

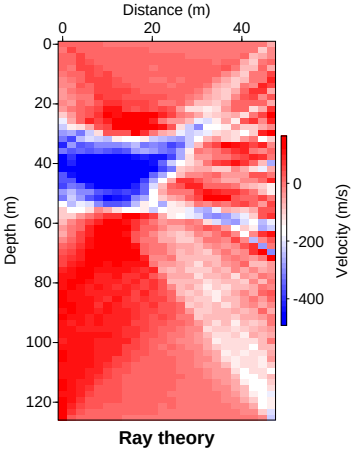

B)

Figure 3: Time-lapse result of traveltime delay tomographic inversion. A) Velocity difference structure compiled from scattering theory. B) Velocity difference structure inferred from ray theory.

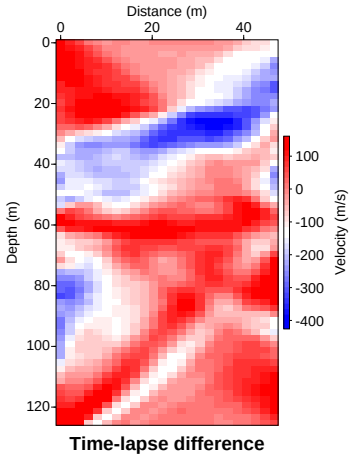

A)

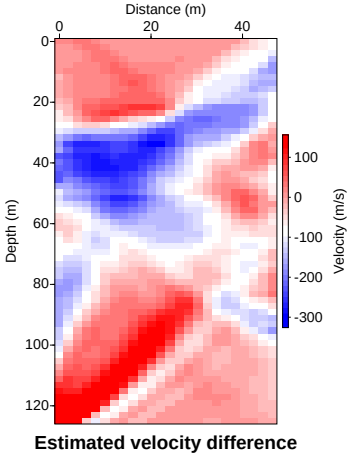

B)

Figure 4: A) Difference velocity tomogram formed by subtracting baseline (pre-flood) image from the post-flood image. B) Difference tomogram created by the last method described in the paper.

ory is applicable in some other geophysical disciplines, such as high-resolution reservoir characterisation, fluid front detection and monitoring of CO_2-sequestration. Currently, we are preparing an scaled ultrasonic experiment for the simulation of CO_2 injection in the subsurface. The time-lapse tomographic method will be applied to monitor induced velocity changes. Time-lapse tomography has been applied to monitor steam injection into tar sand (see another abstract of Spetzler submitted to this conference).

ACKNOWLEDGEMENTS

Šijačić is sponsored through the CATO project and Spetzler is sponsored by the Dutch technology organisation STW, the project no. DAR. 6293. We gratefully acknowledge Neil Goulty and Gerhard Pratt for the permission to use the Durham laboratory data.

REFERENCES

Aki, K. and P. G. Richards, 1980, Quantitative seismology: Theory and methods: W. H. Freeman and Co.

Legget, M., N. R. Goulty, and J. E. Kragh, 1993, Study of traveltime and amplitude time-lapse tomography using physical model data: Geophys. Prosp., **415**, 599–619.

Pratt, G. R., 1999, Seismic waveform inversion in the frequency domain, part 1: Theory and verification in a physical scale model: Geophysics, **64**, 888–901.

Snieder, R. and A. Lomax, 1996, Wavefield smoothing and the effect of rough velocity perturbations on arrival times and amplitude: Geophys. J. Int., **125**, 796–812.

Spetzler, J., 2003a, Comparison of ray theory and finite-frequency wave theory in crosswell tomography: Presented at the 65th.

——— 2003b, Finite-frequency wavefield theory for high-resolution velocity estimation using transmission and reflection data: 73rd, Expanded Abstracts, 2315–2318.

Spetzler, J., C. Sivaji, O. Nishizawa, and Y. Fukushima, 2002, A test of ray theory and scattering theory based on a laboratory experiment using ultrasonic waves and numerical simulations by finite-difference method: Geophys. J. Int., **148**, 165–178.

Spetzler, J. and R. Snieder, 2001, The effects of small-scale heterogeneity on the arrival time of waves: Geophys. J. Int., **145**, 786–796.

Woodward, M. J., 1992, Wave-equation tomography: Geophysics, **57**, 15–26.

EDITED REFERENCES

Note: This reference list is a copy-edited version of the reference list submitted by the author. Reference lists for the 2006 SEG Technical Program Expanded Abstracts have been copy edited so that references provided with the online metadata for each paper will achieve a high degree of linking to cited sources that appear on the Web.

REFERENCES

Aki, K., and P. G. Richards, 1980, Quantitative seismology: Theory and methods: W. H. Freeman and Co.

Legget, M., N. R. Goulty, and J. E. Kragh, 1993, Study of traveltime and amplitude time-lapse tomography using physical model data: Geophysical Prospecting, **415**, 599–619.

Pratt, G. R., 1999, Seismic waveform inversion in the frequency domain, part 1: Theory and verification in a physical scale model: Geophysics, **64**, 888–901.

Snieder, R., and A. Lomax, 1996, Wavefield smoothing and the effect of rough velocity perturbations on arrival times and amplitude: Geophysical Journal International, **125**, 796–812.

Spetzler, J., 2003a, Comparison of ray theory and finite-frequency wave theory in crosswell tomography: 65th Annual Conference and Exhibition, EAGE, Extended Abstracts, F40.

———, 2003b, Finite-frequency wavefield theory for high-resolution velocity estimation using transmission and reflection data: 73rd Annual International Meeting, SEG, Expanded Abstracts, 2315–2318.

Spetzler, J., C. Sivaji, O. Nishizawa, and Y. Fukushima, 2002, A test of ray theory and scattering theory based on a laboratory experiment using ultrasonic waves and numerical simulations by finite difference method: Geophysical Journal International, **148**, 165–178.

Spetzler, J., and R. Snieder, 2001, The effects of small-scale heterogeneity on the arrival time of waves: Geophysical Journal International, **145**, 786–796.

Woodward, M. J., 1992, Wave-equation tomography: Geophysics, **57**, 15–26.